Subpixel Corner Detection Using Spatial Moment[1)]

WANG She-Yang SONG Shen-Min QIANG Wen-Yi CHEN Xing-Lin

(*Department of Control Engineering, Harbin Institute of Technology, Harbin* 150001)

(E-mail: jywsy@hit.edu.cn)

Abstract A novel subpixel corner detection method based on spatial moment is developed in this paper. Firstly, the spatial-moment-generating function, gradient magnitude and variation of gradient-direction corner are used as the decision rule of corner detection by analyzing the mathematical formula of corner-model spatial moment. Then Non-max suppression technique is utilized to detect the vertex of feature corner. Finally, in order to improve its localization performance, subpixel corner detection is implemented by the bilinear interpolation and Newton iteration method. Experiments illustrate that the spatial moment corner detector has better robustness and localization performance than Kitchen detector and Harris detector.

Key words Spatial moment, corner detection, gradient-direction corner, bilinear interpolation

1 Introduction

As a key problem in image processing and computer vision, corner detection has drawn a lot of attention in the past twenty years. Many corner detectors have been reported in open literature. At present there are two main categories of corner detectors: 1) One is to segment the image into regions, and extract the boundaries as a chain code, then identify corners as points where the boundary direction changes rapidly. This approach has been largely abandoned as it relies on the previous segmentation step, which is a complex task itself and is also computationally expensive. 2) The other is to directly detect corner from the gray-level image without any previous segmentation. This method may be classified into two kinds: 1) Image curvature is used to detect the corner. 2) Corner detection is implemented by using intensity variation in every direction. Main methods of the first kind include: Kitchen detector[1] and Wang detector[2]. Kitchen and Rosenfeld introduced a corner detection method based on the change of gradient direction along an edge contour multiplied by the local gradient magnitude. Wang and Brandy proposed a corner detection algorithm based on the measurement of surface curvature. Main methods of the second kind include: Harris detector[3], Moravec detector[4] and Susan detector[5].

All of the methods above use derivatives for detecting corner. Derivatives are sensitivity to noise, therefore, the corner detectors based on image curvature, which utilize second derivatives to compute curvature, can hardly detect corner when noise is strong. Accuracy of feature detection has an important influence on object tracking, pose estimation and camera calibration, so localization performance is a key criterion to evaluate a corner detector. Almost every detector can detect corner point at pixel level, but fails at subpixel level, therefore research on subpixel corner detection is important.

Spatial moment has been used for edge feature detection[6], but not for corner feature detection. This paper derives the decision rule of the corner detection by analyzing the corner model, then utilizes non-max suppression technique to detect the vertex of corner at pixel level; To improve its localization performance, subpixel corner detection is implemented by bilinear interpolation and Newton iteration method.

2 Subpxiel corner detection

2.1 Decision rule of the corner detection

Fig. 1 shows a corner feature model. The gray function of the corner is $f(x, y)$, the corner is defined as 2θ. The two sides of the corner make angles $\varphi + \theta$ and $\varphi - \theta$ with x-axis, where the bisector of the corner makes an angle φ with the x-axis. Also, assume the gray level outside the corner is h and $h + k$ within the corner. Now, the bisector of the corner is the line of symmetry. Thus, if we rotate the corner by angle $-\varphi$, it will be located symmetrical to the x-axis, as shown in Fig. 2. The gray function

1) Supported by the Foundation of the National Ministry of Education
Received July 30, 2004; in revised form June 26, 2005

of the corner after rotation is $f'(x,y)$. The spatial moments of function $f(x,y)$ and function $f'(x,y)$ are given by

$$M_{pq} = \int\int_{x^2+y^2\leqslant 1} x^p y^q f(x,y)\mathrm{d}y\mathrm{d}x \tag{1}$$

$$M'_{pq} = \int\int_{x^2+y^2\leqslant 1} x^p y^q f'(x,y)\mathrm{d}y\mathrm{d}x \tag{2}$$

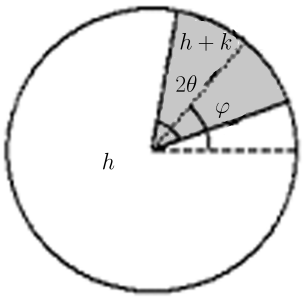

Fig. 1 Corner model

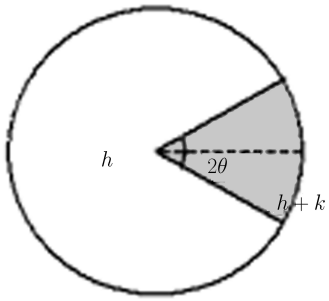

Fig. 2 Corner model after rotation

For a digital image, the spatial moments of the function $f(x,y)$ are calculated by correlating the gray level of image with masks.

For the moments of the two functions we have

$$\begin{aligned}
&M'_{00} = M_{00}\\
&M'_{10} = \cos\varphi M_{10} + \sin\varphi M_{01}\\
&M'_{01} = -\sin\varphi M_{10} + \cos\varphi M_{01}\\
&M'_{20} = \cos^2\varphi M_{20} + 2\cos\varphi\sin\varphi M_{11} + \sin^2\varphi M_{20}\\
&M'_{02} = \sin^2\varphi M_{20} - 20\cos\varphi\sin\varphi M_{11} + \cos^2\varphi M_{20}
\end{aligned} \tag{3}$$

The function $f'(x,y)$ is symmetric about the x-axis, thus, $M'_{01} = 0$, namely, $\tan\varphi = \frac{M_{01}}{M_{10}}$.

Referring to Fig. 2, we can calculate,

$$M'_{00} = \int\int_{x^2+y^2\leqslant 1} f'(x,y)\mathrm{d}x\mathrm{d}y = h\int_0^{2\pi}\int_0^1 \rho\mathrm{d}\rho\mathrm{d}\upsilon + k\int_{-\theta}^{\theta}\int_0^1 \rho\mathrm{d}\rho\mathrm{d}\upsilon = h\pi + k\theta \tag{4}$$

$$\begin{aligned}
M'_{10} = &\int\int_{x^2+y^2\leqslant 1} xf'(x,y)\mathrm{d}x\mathrm{d}y = h\int_0^{2\pi}\int_0^1 \rho\cos(\upsilon)\rho\mathrm{d}\rho\mathrm{d}\upsilon +\\
&k\int_{-\theta}^{\theta}\int_0^1 \rho\cos(\upsilon)\rho\mathrm{d}\rho\mathrm{d}\upsilon = 0 + \frac{2k\sin(\theta)}{3}
\end{aligned} \tag{5}$$

$$M'_{01} = \int\int_{x^2+y^2\leqslant 1} yf'(x,y)\mathrm{d}x\mathrm{d}y = 0 \tag{6}$$

$$\begin{aligned}
M'_{20} = &\int\int_{x^2+y^2\leqslant 1} x^2 f'(x,y)\mathrm{d}x\mathrm{d}y = h\int_0^{2\pi}\int_0^1 \rho^2\cos^2(2\upsilon)\rho\mathrm{d}\rho\mathrm{d}\upsilon +\\
&k\int_{-\theta}^{\theta}\int_0^1 \rho^2\cos^2(2\upsilon)\rho\mathrm{d}\rho\mathrm{d}\upsilon = \frac{\pi}{4}h + \frac{k}{4}\theta + \frac{k}{8}\sin(2\theta)
\end{aligned} \tag{7}$$

$$\begin{aligned}
M'_{02} = &\int\int_{x^2+y^2\leqslant 1} y^2 f'(x,y)\mathrm{d}x\mathrm{d}y = h\int_0^{2\pi}\int_0^1 \rho^2\sin^2(2\upsilon)\rho\mathrm{d}\rho\mathrm{d}\upsilon +\\
&k\int_{-\theta}^{\theta}\int_0^1 \rho^2\sin^2(2\upsilon)\rho\mathrm{d}\rho\mathrm{d}\upsilon = \frac{\pi}{4}h + \frac{k}{4}\theta - \frac{k}{8}\sin(2\theta)
\end{aligned} \tag{8}$$

When the corner model is satisfied, which is shown in Fig. 2, by (4)$\sim$(8) we have

$$2(M'_{20} + M'_{02}) - M'_{00} = 0 \tag{9}$$

$$M'_{20} - M'_{02} = \frac{k\sin(\theta)\cos(\theta)}{2} \tag{10}$$

When the edge model is satisfied, which is shown in Fig. 4, we have[6]

$$2(M'_{20} + M'_{02}) - M'_{00} = \frac{2}{3}kl\sqrt{(1-l^2)^3} \tag{11}$$

$$M'_{20} - M'_{02} = \frac{2}{3}kl\sqrt{(1-l^2)^3} \tag{12}$$

Let $S(x,y) = 2(M'_{20} + M'_{02}) - M'_{00}$. In Fig. 3 and Fig. 4, the radiuses of the two circles are 1 and 0.5, respectively, so $2(x^2+y^2) - 1 < 0$ in the black area, $2(x^2+y^2) - 1 > 0$ in the gray area. In Fig. 3 $\int\int(2x^2 + 2y^2 - 1)\mathrm{d}x\mathrm{d}y$ of the two areas are equal, thus, when the gray level of the black area is the same as the gray area′s,

$$S(x,y) = 0 \tag{13}$$

In Fig. 4 $\iint(2x^2 + 2y^2 - 1)\mathrm{d}x\mathrm{d}y$ of the two areas are not equal, so $S(x,y) \neq 0$ when their gray levels are the same.

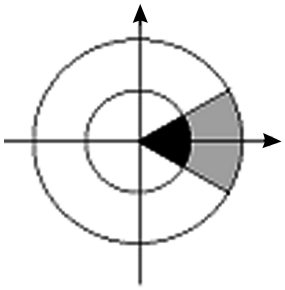

Fig. 3 Corner model

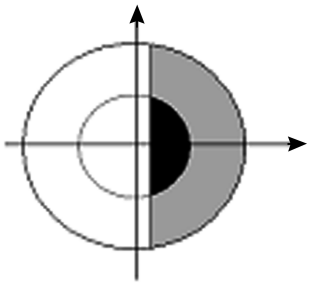

Fig. 4 Edge model

The spatial-moment-generating function $g(x,y)$ is defined as

$$g(x,y) = \frac{|M'_{20} - M'_{02}|}{S(x,y)} \tag{14}$$

At edge points, substitution of (11) and (12) into (14) gives $|g(x,y)| = 1$. At corner points, substitution of (9) and (10) into (14) gives $|g(x,y)| > 1$, hence the feature corner can be detected by function $g(x,y)$.

When the pixel have very little intensity change compared with other pixel around because of noise, $S(x,y)$ is almost equal to 0, thus, $|g(x,y)| > 1$. Because of that, we cannot only make use of function $g(x,y)$ to detect corner. In digital images, corners are formed where two edges meet, and these points correspond to the discontinuity in the direction of gradient vector in a local image neighborhood, gradient-direction variation and gradient magnitude are used for eliminating false corner which results from the noise.

M_{01} and M_{10} can be used as the horizontal component and vertical component of image gradient[6], thus, the gradient magnitude can be given by

$$\mathrm{d}(x,y) = \sqrt{M_{01}^2 + M_{10}^2} \tag{15}$$

The gradient-direction corner ϕ can be defined as

$$\tan\phi = \frac{M_{01}}{M_{10}} \tag{16}$$

Then, the gradient magnitude of the gradient-direction corner $d_\phi(x,y)$ is computed using the Soble mask.

Therefore, the spatial-moment-generating function, gradient magnitude and variation of gradient-direction corner are used as decision rule to detect the corner. When $|g(x,y)| \geqslant k_1$, $d(x,y) > k_2$, and $d_\phi(x,y) > k_3$, where k_1, k_2 and k_3 are thresholds and $K_1 > 1$, pixel (x,y) may be a corner point, otherwise, it is not a corner point.

The decision rule above is not suficient to detect the vertex of corner, therefore, non-max suppression technique is put forward for accurately detecting the vertex.

2.2 Non-max suppression technique

The corner model near vertex is illustrated in Fig. 5. Rotating the corner makes the bisector of the corner coincide with x-axis, which is shown in Fig. 6. The coordinates of the vertex are $(t, 0)$ in the rectangular coordinates. The corner is defined as 2θ. Variation of function $g(x, y)$ with t is shown in Fig. 7.

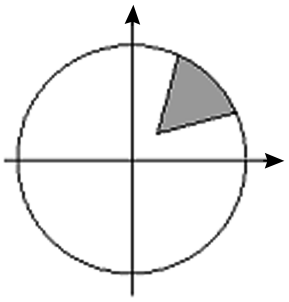

Fig. 5 Corner model near vertex

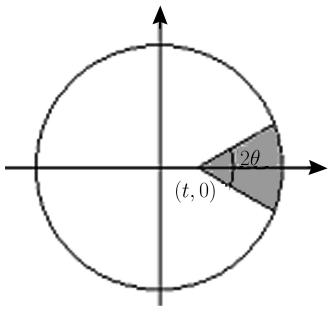

Fig. 6 The neighborhood of corner after rotation

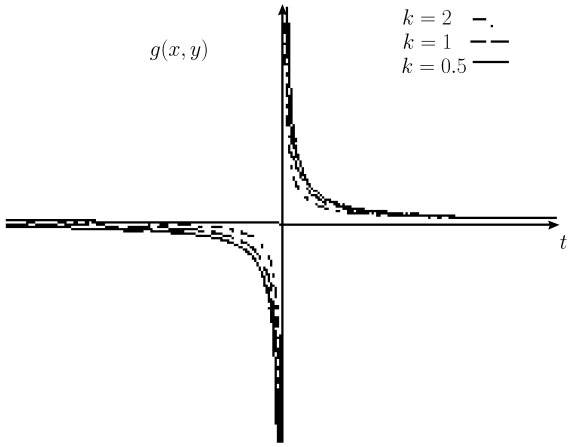

Fig. 7 Variation ofwith

When the feature corner is 2θ, $k = \tan\theta$. Fig. 7 illustrates that $|g(x, y)|$ is an decreasing function with θ, and variation of $|g(x, y)$ with t is not affected by θ. In Fig. 7, if $t < 0$, the pixel is within the corner and $g(x, y) < 0$; if $t > 0$, the pixel is outside the corner and $g(x, y) > 0$. In addition $|g(x, y)|$ is a decreasing function with $|t|$, as illustrated in Fig. 7. Hence, variation of function $g(x, y)$ is very strong at the vertex of corner. Gradient magnitude $d_g(x, y)$ of function $g(x, y)$ can be used for detecting the vertex of corner. For a digital image, the pixel whose gradient magnitude $d_g(x, y)$ is the biggest in the neighborhood of the corner is the vertex of the corner. $d_g(x, y)$ is given by the Soble mask.

The spatial corner detector is summarized below:

1) Compute spatial moments using every mask, then determine function $g(x, y)$, gradient magnitude $d(x, y)$ and gradient-direction corner ϕ by (14), (15), and (16). Finally, use Soble mask to get gradient magnitude $d_\phi(x, y)$ of the gradient-direction corner.

2) If $|g(x, y)| > k_1$, $d(x, y) > k_2$ and $d_\phi(x, y) > k_3$, pixel (x, y) may be the corner point and let its gray-level $I_1(x, y) = 255$; otherwise, the pixel is not a corner point and let $I_1(x, y) = 0$. Therefore, a binary image I_1 is generated.

3) If $I_1(x, y) = 255$, compute $d_g(x, y)$ of every pixel in an 11×11 neighborhood of the pixel using Soble mask. In a 9×9 neighborhood of the pixel (x, y), the pixel (x_1, y_1) is the vertex of the corner on condition that $|d_g(x_1, y_1)$ is the biggest and $I_1(x_1, y_1) = 255$.

2.3 Subpixel feature detection

To improve localization performance of corner detection, subpixel corner detection based on spatial moment is put forward.

Subpixel corner detecion only can be done on the image of which gray function is continuous, thus, the gray-level of subpixel is given by bilinear interpolation as follows.

$$I(x,y) = (1-\alpha)(1-\beta)I(i,j) + \alpha(1-\beta)I(i+1,j) + (1-\alpha)\beta I(i,j+1) + \alpha\beta I(i+1,j+1) \quad (17)$$

where $i < x < i+1, j < y < j+1, \alpha = x-i, \beta = y-j$, and $I(i,j)$ is the gray function of image.

If a subpixel corner point is determined by function $g(x,y)$, $d_g(x,y)$ must be optimized using higher derivatives for which the calculation is complex and sensitivity to noise. To improve the robustness of corner detection, subpixel corner detecion is implemented by function $S(x,y)$. By (13) and Fig. 7, $S(x,y)$ of the vertex is equal to zero, but $S(x,y)$ of other pixel is not zero near the vertex, therefore, subpixel corner point is determined by Newton iteration method as in (18).

$$x' = x - S(x,y)/d_{sx}(x,y), \quad y' = y - S(x,y)/d_{sy}(x,y) \quad (18)$$

where, the initial values of (x,y) are the vertex of the corner at pixel level. $d_{sx}(x,y)$ and $d_{sy}(x,y)$ are first partial derivatives of function $S(x,y)$. Subpixel corner point is accurately determined within 10 iterations.

3 Example

In this section, we give some experimental results obtained by running some corner detectors on the synthetic and real images.

In order to compare the robustness and localization performance of detectors, we have conducted an experiment on a 120×120 synthetic image. In the image there are 90°, 45°, and 135° corners. Fig. 8 shows the results of the spatial moment detector, Kitchen detector and Harris detector on origin and noisy images. On the origin image, all the three methods can detect feature corners. When the image is corrupted by salt noise and white noise, the result of Kitchen detector is the worst, and the spatial moment detector′s is the best. From Table 1 we can make a conclusion that the localization performance of spatial moment is better than Harris on origin and noisy images. Fig. 8 and Table 1 illustrate the spatial moment detector has better robustness and localization performance than Kitchen detector and Harris detector.

Table 1 Result of the synthetic experiment

	Kitchen	Harris	Spatial	Subpixel on origin image		Subpixel on image with salt noise	
				Harris	Spatial	Harris	Spatial
(10,10)	(10,10)	(11,10)	(10,10)	(9.297,9.558)	(9.182,9.371)	(9.225,9.501)	(9.283,9.3548)
(30,10)	(31,10)	(30,10)	(30,10)	(30.442,9.558)	(30.500,9.500)	(31.532,8.576)	(30.453,9.481)
(50,10)	(50,10)	(50,10)	(50,10)	(49.558,10.558)	(49.500,9.500)	(49.670,8.388)	(49.603,9.612)
(90,10)	(90,10)	(90,10)	(90,10)	(90.702,9.558)	(90.622,9.182)	(89.144,9.492)	(90.598,9.186)
(30,30)	(29,30)	(30,29)	(30,30)	(30.442,30.702)	(30.818,30.629)	(30.649,30.3543)	(30.898,30.891)
(70,30)	(71,30)	(70,30)	(70,30)	(69.923,30.531)	(70.489,30.282)	(70.469,30.5053)	(70.275,30.160)
(30,50)	(30,50)	(30,51)	(30,50)	(49.558,30.442)	(30.818,49.371)	(30.473,49.580)	(30.861,49.029)
(60,60)	(60,60)	(60,60)	(60,60)	(59.558,59.558)	(59.500,59.500)	(59.480,59.506)	(59.338,59.3.03)
(99,60)	(100,60)	(99,60)	(99,60)	(99.558,59.558)	(99.500,59.500)	(100.546,59.614)	(99.437,59.484)
(90,70)	(91,70)	(90,70)	(90,70)	(90.442,69.558)	(90.499,69.501)	(90.3163,69.577)	(90.482,69.473)
(99,100)	(99,100)	(99,100)	(99,100)	(99.442,100.442)	(99.500,100.500)	(99.350,100.508)	(99.542,100.661)
(10,110)	(11,110)	(10,109)	(10,110)	(9.558,110.702)	(9.182,110.629)	(12.473,109.828)	(9.317,110.512)
Errors	(0.5,0)	(0.1,0.25)	(0,0)	(0.058,0.058)	(0.003,0.003)	(0.68,0.89)	(0.11,0.12)

Other experiment has been conducted to calibrate camera parameters. The experiment utilizes a PULNiX CCD camera to acquire image, the image size is of 768×576, and the experiment mask is shown in Fig. 9. In the experiment, Zhang′s calibration method[7] is employed and feature points are the corners of the square, which are detected by the spatial moment detector and Harris detector. The result is shown in Table 2 and Fig. 10. In Table 2, f is the focal distance of the camera, dx and dy are distances between adjacent pixels in the horizontal and vertical directions of the CCD plane, (u,v) are coordinates of image center in the frame buff. k_1, k_2, k_3 and k_4 are distortion coefficients. Fig. 10 shows image coordinate errors between detected feature points and points after mapping. The errors

of Harris detector and the moment spatial detector are respectively denoted by "o" and "+" in Fig. 10, error variance of Harris detector is (0.2290,0.2867), the spatial moment detector′s is (0.1658,0.1747).

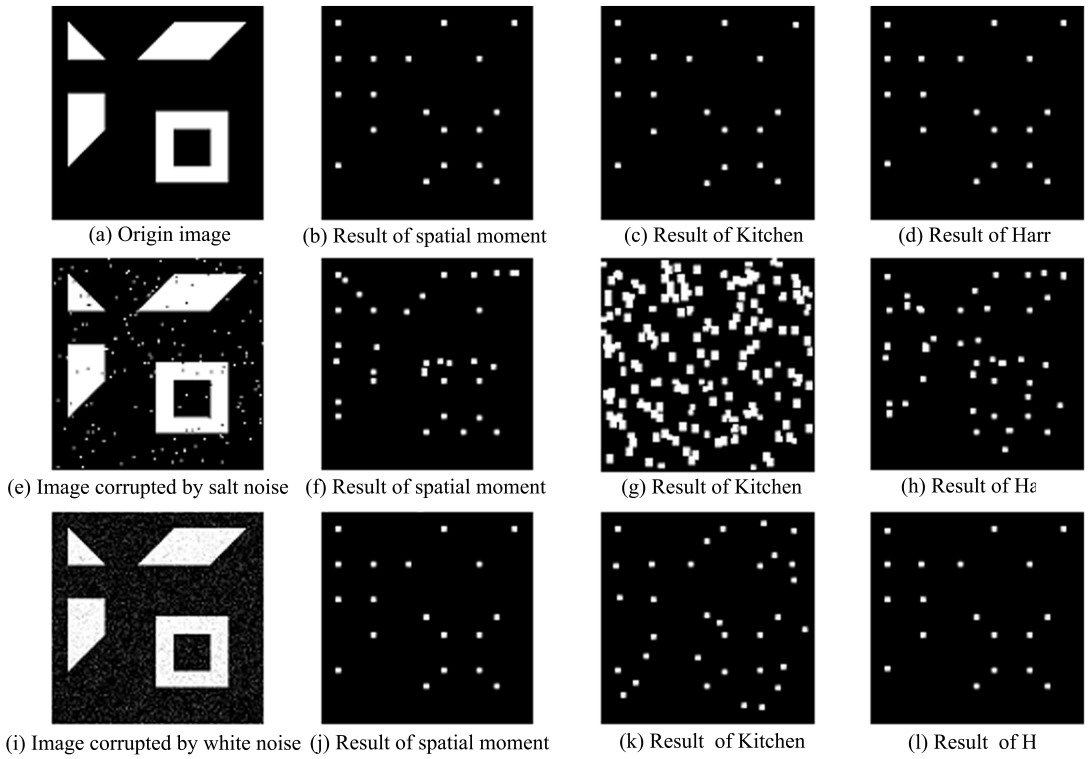

Fig. 8 Result of experiment

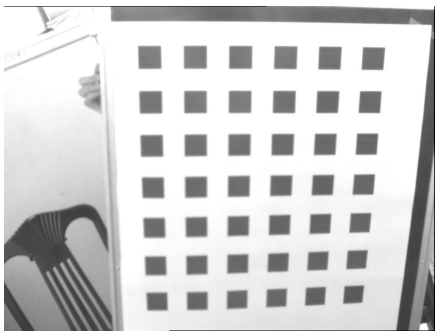

Fig. 9 Calibration mask

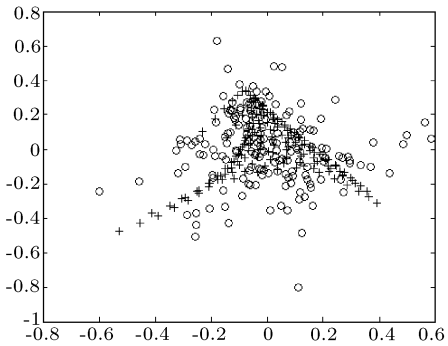

Fig. 10 Errors of detected feature points and points after mapping

Table 2 Camera parameters

	Spatial	Harris
$f/\mathrm{d}x$	1035.9727	1059.76838
$f/\mathrm{d}y$	1026.5845	1055.41493
u	411.3085	414.98034
v	282.1480	285.52993
k_1	−0.01939	−0.19360
k_2	0.18033	0.18410
k_3	0.00128	−0.00004
k_4	0.00028	0.00407
Variance	(0.1658,0.1747)	(0.2290,0.2867)

4 Conclusion

A novel subpixel corner detection method is developed in this paper. It utilizes spatial moment to detect corner points. Because spatial moments are computed by integrating, the spatial moment detector is more robust than other methods. Spatial-moment-generating function changes intensively at the vertex of corner, thus, using gradient of this function can accurately detect the vertex of feature corner. In order to improve its localization performance, subpixel corner detection is implemented by bilinear interpolation and Newton iteration method. The subpixel point is determined by solving equation, in which only first derivative is used, therefore the method has better robustness and localization performance. This method has been applied to vision system of HIT-IV biped robot successfully.

References

1 Kitchen L, Rosenfeld A. Gray level corner detection. *Pattern Recognition Letters*, 1982, **1**(1): 95∼102
2 Wang H, Brandy M. A practical solution to corner detection. In: Proceedings International Conference on Image Processing, Austin, Texas, USA: IEEE Computer Society, 1994. **1**: 919∼923
3 Harris C, Stephens M. A Combined Corner and Edge Detector. In: Proceedings of The Fourth Alvey Vision Conference, Manchester: University of Manchester, 1988. 147∼151
4 Moravec H P. Towards automatic visual obstacle avoidance. In: Proceedings of International Joint Conference on Artificial Intelligence, Cambridge: MIT Press, 1977. 584
5 Smith S M, Brady J M. SUSAN—A new approach to low level image processing. *International Journal of Computer Vision*, 1997. **23**(1): 45∼78
6 Edward P, Lyvers, Mark L, Akey. Subpixel measurements using a moment-based edge operator. *IEEE Transactions on Pattern Analysis and Machine Intelligence*, **11**(12): 1293∼1309
7 Zhang Z. Flexible camera calibration by view a plane from unknown orientation. In: Proceedings of IEEE International Conference on Computer Vision, Corfu, Greece: IEEE Computer Society Press, 1999. 666∼673

WANG She-Yang Received his bachelor and master degrees from Harbin Institute of Technology in 2000 and 2002, respectively. His research interests include pattern recognition, intelligent control, and vision guided robot navigation.

SONG Shen-Min Received his Ph. D. degree from Harbin Institute of Technology in 1996. His research interests include robot vision, robust control, and intelligent control.

QIANG Wen-Yi Professor in the Department of Control Science and Engineering at Harbin Institute of Technology. His research interests include intelligent control, humanoid walking robot, and computer vision.

CHEN Xing-Lin Received his master and Ph. D. degrees in 1991 and 1994, respectively. His research interests include intelligent control, humanoid walking robot, and computer vision.